



1 **The impact multi-decadal of changes in VOCs speciation on urban**
2 **ozone chemistry: A case study in Birmingham, United Kingdom.**

3 Jianghao Li^{1,2}, Alastair C. Lewis^{1,3}, Jim R. Hopkins^{1,3}, Stephen J. Andrews^{1,3}, Tim Murrells⁴, Neil
4 Passant⁴, Ben Richmond⁴, Siqi Hou⁵, William Bloss⁵, Roy Harrison^{5,6}, Zongbo Shi⁵.

5 ¹Wolfson Atmospheric Chemistry Laboratories, University of York, York YO10 5DD, UK

6 ²School of Water and Environment, Chang'an University, Xi'an 710064, China

7 ³National Centre for Atmospheric Science, University of York, Heslington, York YO10 5DD, UK

8 ⁴Ricardo Energy and Environment Gemini Building, Fermi Avenue, Harwell, Oxon OX11 0QR, UK

9 ⁵School of Geography, Earth and Environmental Sciences, University of Birmingham, Edgbaston,
10 Birmingham B15 2TT, UK

11 ⁶Department of Environmental Sciences, Faculty of Meteorology, Environment and Arid Land
12 Agriculture, King Abdulaziz University, P.O. Box 80208, Jeddah 21589, Saudi Arabia

13 *Correspondence to:* Jianghao Li (cfm531@york.ac.uk)

14

15 **Abstract** Anthropogenic non-methane volatile organic compounds (VOCs) in the United Kingdom
16 have been substantially reduced since 1990, partly attributed to controls on evaporative and vehicle
17 tailpipe emissions. Over time other sources with a different speciation, for example alcohols from
18 solvent use and industry processes, have grown in both relative importance and in some cases in
19 absolute terms. The impact of this change in speciation and the resulting photochemical reactivities
20 of VOCs are evaluated using a photochemical box model constrained by observational data during
21 a summertime ozone event (Birmingham, UK), and speciation and apportionment of sources based
22 on the UK national atmospheric emission inventory (NAEI) data over the period 1990-2019. Despite
23 road transport sources representing only 3.3% of UK VOC emissions in 2019, it continued as the
24 sector with the largest influence on local O₃ production rate (P(O₃)). Under case study conditions,
25 the 96% reduction in road transport VOC emissions that has been achieved between 1990 – 2019
26 has likely reduced daytime P(O₃) by ~1.67 ppbv h⁻¹. Further abatement of fuel fugitive emissions
27 was modeled to have had less impact on P(O₃) reduction than abatement of VOCs from industrial
28 processes and solvent emissions. The long-term trend of increased emissions of ethanol and
29 methanol have somewhat weakened the benefits of reducing road transport emissions, increasing



30 P(O₃) by ~0.19 ppbv h⁻¹ in the case study. Abatement of VOC emissions from multiple sources has
31 been a notable technical and policy success in the UK, but some future benefits (from an ozone
32 perspective) of the phase out of internal combustion engine passenger cars may be offset if domestic
33 and commercial solvent emissions of VOCs were to continue to increase.

34

35 **1. Introduction**

36 Elevated tropospheric ozone (O₃) has been a long-standing pollutant of concern in the rural
37 and sub-urban environment and is now becoming more prevalent in urban centers as primary NO
38 traffic emissions reduce (Sicard, 2021). As an important tropospheric oxidant and greenhouse gas
39 (Kumar et al., 2021), exposure to O₃ also increases risks of mortality from respiratory diseases and
40 adversely impacts on crop productivity (Lefohn et al., 2018). O₃ is mainly formed through
41 photochemical reactions involving the oxidation of volatile organic compounds (VOCs) in the
42 presence of nitrogen oxides (NO_x, NO_x=NO+NO₂) (Calvert et al., 2015). The release of VOCs arises
43 from a wide range of activities, including unburned fuel or partially combusted products in exhaust,
44 from solvents used in industry and numerous other diffuse domestic and commercial sources (He et
45 al., 2019). Effective policies to mitigate ozone pollution rely on an accurate estimate of both
46 emissions and speciation of O₃ precursors.

47 The challenge in reducing O₃ lies in its non-linear relationship with its precursors and that
48 individual VOCs have unique capacities for forming ozone. Decades of modelling studies have
49 established regimes where reductions in NO_x or VOCs emissions would be preferentially beneficial
50 to mitigate O₃ – so-called NO_x-limited or VOC-limited regimes (Ivatt et al., 2022; Seinfeld and
51 Pandis, 2016). Abatement of VOCs sources is important in VOCs-limited areas, since decreasing
52 the emissions can effectively reduce the local O₃ production rate, and help limit O₃ peak
53 concentrations (Gaudel et al., 2020). The wide range of sources, including many that are diffuse and
54 occur indoors, and differing photochemical reactivities further complicates O₃ reduction strategies.
55 Different mixes of sources and speciation can lead to need for localized policies. For example, short-
56 chain alkanes and alkenes with high reactivity with hydroxyl radical from on-road transportation in
57 China, have been reported as responsible for 26% of national O₃ formation (Wu and Xie, 2017).
58 Recent research in Los Angeles, the United States showed that release of oxygenated VOCs



59 (OVOCs) from volatile chemical product usage contributed as much as 9 ppb to daytime O₃ (Qin et
60 al., 2021). A field observation study in Delhi, India revealed that the O₃ production in that city was
61 most sensitive to monoaromatics, followed by monoterpenes and alkenes (Nelson et al., 2021).
62 There is therefore no one-size-fits all in terms of which VOCs to target for optimal O₃ abatement
63 efforts.

64 Policy and regulation aimed at improving air quality in many countries including the United
65 States, the United Kingdom and Europe have led to decades of falling VOCs emissions (Lewis et
66 al., 2020; Coggon et al., 2021). This reduction can be substantially attributed to the successful
67 technical implementation of tailpipe exhaust after-treatment technology for gasoline vehicles
68 controls on evaporative emissions from vehicles including during re-fueling and a more widespread
69 set of efforts to control industrial emissions (Winkler et al., 2018). Despite these successes, O₃
70 remains a pollutant of concern; whilst the peak concentrations during O₃ events have reduced in the
71 UK, increases in the long-term urban background O₃ concentrations have been observed since the
72 1990s (Department for Environment, Food & Rural Affairs, 2023). A variety of explanations have
73 been given to account for the increase, including a rising northern hemisphere background O₃,
74 increasing methane which contributes to both global radiative forcing and enhances O₃ production
75 (Tarasick et al., 2019; Abernethy et al., 2021), the increases in non-vehicular sources of VOCs
76 emissions (McDonald et al., 2018; Yeoman and Lewis, 2021), and the reduction of NO_x in VOCs-
77 limited urban areas leading to greater O₃ production efficiency (Diaz et al., 2020).

78 The UK National Atmospheric Emissions Inventory (NAEI) for VOCs has shown increases in
79 relative contribution of solvent usage and the food & wine industry to total national VOCs emission
80 over 1990-2019, and steady growth in the relative importance of OVOCs within the overall
81 speciation (Lewis et al., 2020). Substantial OVOCs emissions can come from unexpected places.
82 For example, alcohols emitted from use of windshield fluid are now estimated to be a larger VOC
83 source from road transport than VOCs from the tailpipe in the UK (Cliff et al., 2023). What effect
84 this shift in speciation is having on ozone chemistry is less well studied. One challenge has been the
85 lack of routine measurement of OVOCs in the national air quality monitoring networks (Air Quality
86 Expert Group, 2020).

87 In this study we evaluate the effects of changing VOCs speciation on urban ozone chemistry,
88 using recent field measurements of O₃ and its key precursors such as NO_x, CO, speciated VOCs and



89 OVOCs in Birmingham, UK during August 2022, and changing speciation and relative amounts of
90 VOCs based on long-trends in the NAEI. The sensitivity of *in-situ* production and OH reactivities
91 of the measured O₃ precursors are investigated by constraining the observational data sets to a zero-
92 dimensional chemical box model. By incorporating the detailed NAEI VOCs emission inventories
93 over the period of 1990-2019 into the model, O₃ formation in Birmingham is used as a case study
94 to quantify the impacts of the real-world changes in VOCs sources on urban O₃ production rate. The
95 relative importance of different VOCs functional group classes on the O₃ production are also
96 evaluated.

97

98 **2. Materials and Methods**

99 2.1 Field observations

100 The observations are taken from the Birmingham NERC Air Quality Supersite during August
101 2022. This is located on the University of Birmingham (52°27'20.2"N 1°55'44.3"W) campus. The
102 site has been in operation for many years, and represents an urban background environment; it is
103 influenced by transport emissions from nearby arterial roads and residential emissions from
104 surrounding area. There are no significant industrial activities within a 4km radius of the site.

105 Continuous measurements of NO, NO₂, CO, CH₄, VOCs, O₃, along with meteorological
106 parameters including air temperature and pressure, relative humidity, wind speed and direction were
107 made. Briefly, NO and NO₂ were measured by a chemiluminescence-based T200 analyzer (Teledyne
108 API, U.S.A.) and the T500U Cavity Attenuated Phase Shift (CAPS) analyzer (Teledyne API,
109 U.S.A.). The concentration of NO_x was then the statistical sum of NO and NO₂. The mixing ratio of
110 CO were measured by a laser absorption spectroscopy Multi-species Continuous Emissions
111 Monitoring instrument (Enviro Technology Service Ltd., UK) (Li et al., 2020). Manual calibration
112 and span checks for the above instruments were performed every 3 days, and automatic zero
113 calibration was set on daily bases. O₃ was measured by an O₃ analyzer (Model 49i, Thermo Fisher
114 Scientific Inc., U.S.A.) with a minimum detection limit (MDL) of 1.0 ppbv. Meteorological
115 parameters including air temperature and pressure, and relative humidity were obtained from a
116 weather station WS300-UMB weather station (Luff GmbH, Germany). Additionally, Wind speed
117 and direction were measured by a 3-axis ultrasonic anemometer (Gill Instruments Ltd., UK) over



118 the campaign.

119 A gas chromatography-flame ionization detection (GC-FID) analysis system (7890A, Agilent
120 Technologies, U.S.A.) was used to quantify 38 individual VOCs species. Details on instrument
121 settings and quality assurance/quality control methods can be found in (Warburton et al., 2023).
122 Briefly, the GC-FID system utilizes dual detectors for C₂–C₉ compounds. Ambient samples were
123 dried at –40 °C using a water trap and then VOCs pre-concentrated on a carbon adsorbent. Once a
124 0.5L sample had been collected, a pre-concentration trap was warmed slightly from –120 °C to
125 –80 °C to purge trapped atmospheric CO₂. The trap was then heated to 190 °C for 3 minutes with a
126 counter flow of helium thermally desorbing the concentrated VOCs onto focusing micro-trap held
127 at –120 °C. The analytes were flash heated and passed onto a VF-WAX column. The unresolved
128 analytes were then transferred into a Na₂SO₄-deactivated Al₂O₃ porous-layer open tubular (PLOT)
129 column via a Dean switch, for separation and detection by the first FID. The Dean switch then
130 diverted the analytes onto a fused silica internal diameter to balance column flows and subsequently
131 split VOCs and oxygenated VOCs into the second FID. Quantification of C₂–C₆ hydrocarbons was
132 completed by the first FID. Quantification of C₇–C₉ hydrocarbons and oxygenated VOCs was
133 completed by the second FID. Most of the measured species were directly calibrated using 4 ppbv
134 gas standard cylinders (the National Physical Laboratory, Teddington, UK). The calibration for
135 acetone, acetaldehyde, ethanol, and methanol were processed by using effective carbons with
136 reference to toluene. In this study, the concentration of total VOC (TVOC) was defined as the
137 statistical sum of concentrations of measured individual species, but this is not meant to infer that
138 this represents the total reactive carbon in air, which would always be greater than this value due to
139 unmeasured species. Later in this study we broadly group species according to their chemical
140 function groups, summing into alcohols, ketones, alkanes, alkenes, aromatics, aldehydes, and
141 alkynes.

142 2.2 National emission inventory for VOCs

143 Estimates of UK anthropogenic VOC emissions are taken from the NAEI. The NAEI uses a
144 combination of UK-specific methods and default methods as recommended in the European
145 Monitoring and Evaluation Programme (EMEP)/European Environment Agency (EEA) Emission
146 Inventory Guidebook (European Environment Agency, 2016). Further details can be found in (NAEI,
147 2021). The VOC inventory is also disaggregated into inventories for each individual VOC species



148 and details of the speciation process and assumptions can be found in (Passant, 2002) and (Lewis et
149 al., 2020).

150 Methods to estimate emissions can be divided into two groups: those using emission factors,
151 and those using ‘point source’ emissions data reported to regulators by the operators of individual
152 industrial sites. The emission factor methods require UK activity data, for example consumption of
153 paint, consumption of a fuel, production of steel or vehicle kilometers travelled. The activity data is
154 then combined with an emission factor which expresses the total VOC emission that is expected per
155 unit of a given activity. Most total VOC emission factors are taken from the internationally applied
156 EMEP/EEA Emission Inventory Guidebook and so are not necessarily UK-specific. The factors for
157 road transport are directly calculated for the UK and a particularly detailed approach is used to
158 estimate emissions using emission factors from the Guidebook for many different vehicle types and
159 emission standards, fuels and road types combined with detailed transport activity from the UK
160 Department for Transport. Government statistics cannot always provide the necessary activity data
161 for other sectors, so industry data are used instead. For instance, NAEI data on consumption of
162 products containing organic solvents are from industry sources. The alternative point source method
163 can be used for source categories where emissions data can be obtained for all sites within the sector,
164 and this limits the method to source categories such as crude oil refining, steel production and
165 chemicals production. The emissions data reported by the operators of these sites can be based on
166 emissions monitoring, although this is not always the case and emissions might instead be estimated,
167 for example, using emission factors.

168 The NAEI produces updates to the inventory for total VOC mass emissions by source sector
169 each year to achieve a consistent historic time-series reflecting trends in UK emissions. Emissions
170 of individual VOC species are estimated using source-specific speciation profiles which show the
171 mass fraction of each species, or in some cases groups of species, emitted by the source (NAEI,
172 2021; Passant, 2002). Over 600 individual VOC species or species groups are included in the
173 speciation, based on sources in industry, regulators and in some cases literature sources and
174 databases such as the USEPA SPECIATE database. The speciated inventory tends to be more
175 uncertain than the estimation of total mass of VOC emissions. The inventory for total VOC mass is
176 updated annually, whereas the speciation profiles are only periodically updated when new
177 information becomes available. Thus, trends in a particular species for a sector are a reflection of



178 changes in total VOC emissions for the sector and do not normally reflect any changes over time in
179 the speciation profile of the sector which may have occurred.

180 2.3 Photochemical box model

181 The framework for evaluating effects of changing VOCs speciation is a 0-D Atmospheric
182 Modelling chemistry box model (Wolfe et al., 2016), driven by the Version 3.3.1 of the Master
183 Chemical Mechanism (MCM v3.3.1) (Saunders et al., 2003; Jenkin et al., 2003). The model can be
184 effective in identifying the instantaneous *in-situ* O₃ sensitivity to changes in individual VOCs. The
185 measured concentrations of 38 VOCs species, NO_x, and CO, along with air temperature and pressure,
186 and relative humidity were averaged to a time resolution of 1-hour to constrain the model. A 3-day
187 model spin-up, with each 24-hour model run constrained by the observational data, was performed
188 in order to initialize the unmeasured compounds and transient radicals. The modelled outputs on the
189 4th day were taken as representing steady state of the photochemistry.

190 Photolysis rates were calculated as a function of solar zenith angle (Saunders et al., 2003):

$$191 \quad J = I(\cos \chi)^m \exp(-n \sec \chi) \quad (1)$$

192 Where J is the photolysis rate in s⁻¹; l , m , n are constants derived from radiative transfer model
193 runs for clear sky condition at an altitude of 0.5 km and literature cross sections/quantum yields; χ
194 is the solar zenith angle in radians.

195 The net production rate of O₃ ($P(O_3)$) is calculated by the difference of the production rate of
196 O₃ and the destruction rate of O₃, as in Equation (2):

$$197 \quad P(O_3) = (k_{HO_2+NO}[HO_2][NO] + \sum_i k_{RO_2_i+NO}[RO_2][NO]) - \\ (k_{O^1D+H_2O}[O^1D][H_2O] + k_{O_3+OH}[O_3][OH] + k_{O_3+HO_2}[O_3][HO_2] \\ k_{NO_2+OH}[NO_2][OH] + \sum_i k_{RO_2_i+NO_2}[RO_2][NO_2]) \quad (2)$$

198 Where the former part is the rate of O₃ production, representing by rate of NO oxidation by
199 HO₂ and RO₂ radicals; the latter part is the destruction rate of O₃, calculating by the sum of the rate
200 of O₃ photolysis, the rates of the reactions with OH and HO₂ radicals, and the rates of NO₂ loss
201 through reactions with OH and RO₂ radicals.

202 The sensitivity of O₃ to its precursors is quantified by the index of relative incremental
203 reactivity (RIR) (Liu et al., 2022b), as in Equation (3):

$$204 \quad RIR = \frac{\Delta P(O_3)}{P(O_3)} \times a^{-1} \quad (3)$$



205 Where RIR is the Relative Incremental Reactivity in %/%, $\Delta P(O_3)/P(O_3)$ is the ratio of the
206 change in O_3 production rate to the base O_3 production rate; a is the reduction percentage in the
207 input concentration of O_3 precursors – a factor that allows for the effects of changing absolute
208 amounts of VOCs to be evaluated. Here a value of 30% was adopted for a .

209

210 **3. Results and Discussion**

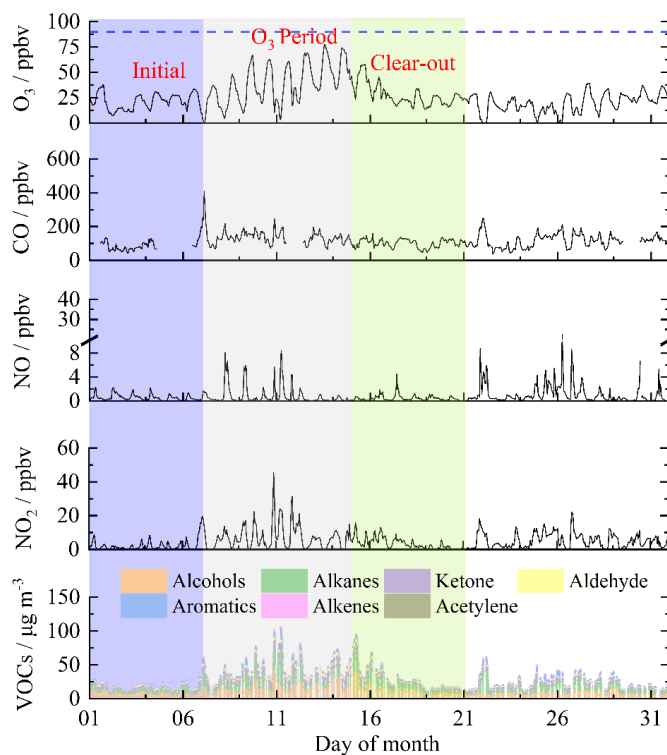
211 3.1 Observation overview

212 The time series of O_3 and its precursors during August 2022 are shown in Figure 1, subdivided
213 into periods that will be referred to as ‘initial period’, ‘ O_3 period’, and ‘clear-out’. The three periods
214 covered 1st August-21th August 2022. Each period included one full week to avoid
215 weekday/weekend differences in NO_x and VOCs concentrations impacting differently when O_3
216 production was compared between the three periods (de Foy et al., 2020). Ozone showed a generally
217 increasing trend from 1st to 14th August and then returned to relatively low concentrations after 15th
218 August 2022. The daily maximum 8 h average O_3 concentrations (MDA8h O_3) during the O_3 period
219 exceeded the WHO guideline value ($100 \mu g m^{-3}$), ranging from 111 to $153 \mu g m^{-3}$. The elevated O_3
220 during the middle of the month corresponded to more intense photochemical formation under hot
221 weather conditions ($32.7^\circ C$ in maximum) and higher concentrations of O_3 precursors (Table S1).

222 The diurnal profile of NO and NO_2 in the three periods generally showed a bimodal pattern,
223 albeit less pronounced in the initial and clear-out periods (Figure 2). The two peaks likely arise as
224 a consequence of increased traffic volumes at the start and end of the day, coupled to boundary layer
225 height changes in the early morning and into the evening (Lee et al., 2020). The average
226 concentrations of NO_2 during 05:00-10:00 were 10.8 ppbv in the O_3 period, which was considerably
227 higher than the concentration of 3.9 ppbv in the initial period and 3.4 ppbv in the clear-out period.
228 The low level of NO in the O_3 period highlights the rapid consumption of NO via photochemical
229 processes. The oxidation of CO is an important source of HO_2 in the atmosphere (Chen et al., 2020),
230 here in the range of 82.5 to 134.2 ppbv with little difference between periods. The diurnal profiles
231 of O_3 peaked at 15:00, with maximum hourly concentrations of 31.6, 67.2, and 30.4 ppbv in the
232 initial, O_3 , and clear-out periods, respectively. Slight decreases in O_3 were observed during
233 nighttime (00:00-05:00), indicating enhanced NO titration effects.



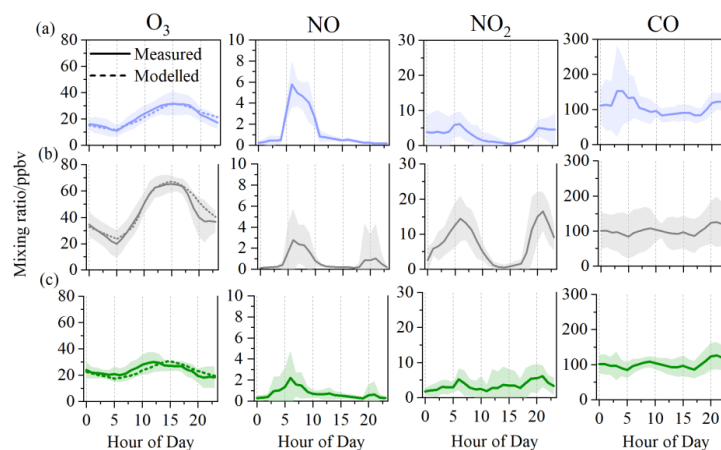
234 The detailed VOCs composition in the three periods is presented in Figure S1. Concentration
 235 of TVOC were 19.4 ± 8.4 , 48.0 ± 18.8 , and $23.5 \pm 12.5 \mu\text{g m}^{-3}$ in the three periods, respectively.
 236 Alcohols, represented mainly by methanol and ethanol, were the predominant group that contributed
 237 40.3% - 47.4% of over measured VOCs mass. This was followed by alkanes (21.4%-24.6%) and
 238 ketones (16.3%-17.3%). Contributions of aldehyde (acetaldehyde), aromatics, alkenes, and
 239 acetylene were low, ranging from 1.0% to 9.4% of total mass. Ambient VOCs largely influenced by
 240 combustion-related sources (i.e., vehicle exhaust and coal combustion) generally show alkane-
 241 dominated composition (Wu and Xie, 2017). Here, the composition and amount of VOCs observed
 242 were most likely influenced by non-combustion processes such as volatile chemical product usage
 243 and industrial processes (Gkatzelis et al., 2020). Methanol was the most abundant VOC with an
 244 average concentration of 4.1 ppbv, followed by acetone (2.0 ppbv), ethane (1.9 ppbv), ethanol (1.8
 245 ppbv), and acetaldehyde (1.0 ppbv). The average ratio of ethene/ethane was 0.2 ± 0.1 over the
 246 campaign, considerable lower than seen in polluted locations, e.g. Hong Kong (China) (0.7 ± 0.1)
 247 (Wang et al., 2018) and Seremban (Malaysia) (1.1) (Zulkifli et al., 2022).



248



249 Figure 1. Time series of O₃, CO, NO, NO₂, and VOCs groups at the Birmingham Supersite. The
 250 blue dash line denotes the national standard (90 ppbv) for hourly O₃ concentration.
 251



252
 253 Figure 2. Diurnal variations of O₃, NO, NO₂, and CO during the initial (a), O₃ period (b), and
 254 clear-out period (c). The shaded areas represent standard variations.
 255

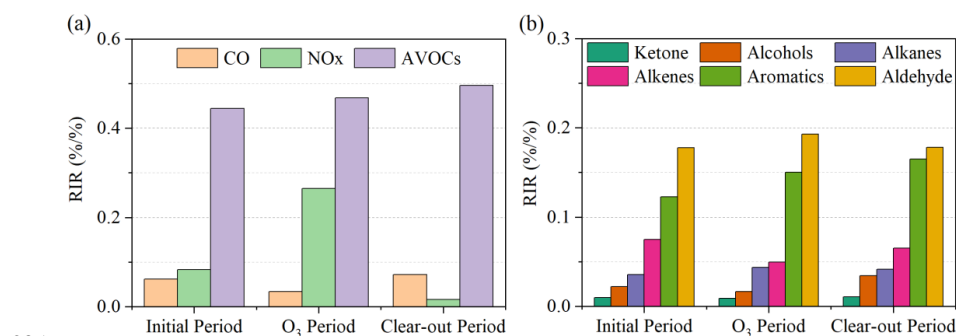
256 3.2 Observation-based O₃ formation sensitivity

257 The *in-situ* O₃ formation sensitivity was examined via reaction rates of ozone precursors and
 258 OH radical (OH reactivities, $k(\text{OH})$) and RIR scales of ozone precursors, along with the chemical
 259 budgets of O₃ formation and loss. In initial and clear-out periods, $k(\text{OH})$ exhibited consistent diurnal
 260 patterns, ranging from 2.4 to 5.9 s⁻¹ (Figure S2). In the O₃ period, $k(\text{OH})$ reached 9.0 and 8.7 s⁻¹ at
 261 approximately 07:00 and 20:00, respectively. A rapid increase in $k(\text{OH})$ was observed in the early
 262 morning (00:00-06:00). VOCs and model generated species represented 60.5%, 65.7%, and 56.7%
 263 of the total $k(\text{OH})$ in the three periods, respectively. NO_x and CO only contributed 10.2% -27.9% to
 264 total $k(\text{OH})$. Among of the VOCs groups, alcohols exhibited the largest $k(\text{OH})$ in all periods,
 265 accounting for 5.0% - 6.9% of the total $k(\text{OH})$. The diurnal production and loss of O₃ are shown in
 266 Figure S3. The oxidation and photolysis of VOCs promoted the production of RO₂, and NO+RO₂
 267 contributed 47.7% of the O₃ production pathways in the O₃ period and 36.2% and 39.8% in initial
 268 and clear-out periods, respectively. Considering O₃ destruction, OH+NO₂ was the most important
 269 pathway during morning (08:00-12:00), accounting for 73.5%, 55.4% and 59.4% of the O₃
 270 destruction pathways in the three periods. The dominant OH+NO₂ contribution to O₃ destruction
 271 suggested that the *in-situ* O₃ productions in all three periods was sensitive to VOCs emissions to



272 some extent.

273 The relative incremental reactivity of NO_x, CO, and anthropogenic VOCs (AVOCs, all
 274 measured VOCs except for isoprene) are shown in Figure 3. The *in-situ* O₃ production was most
 275 sensitive to anthropogenic VOCs with the highest positive RIR values (0.44 - 0.49). This is as
 276 anticipated given earlier analyses demonstrating their role in determining *k*(OH) and O₃ production.
 277 The low RIR (0.03 - 0.07) for CO in all three periods indicated a minor contribution of CO oxidation
 278 to O₃ production. The high RIR (0.24) for NO_x was only observed in the O₃ period. Acetaldehyde
 279 showed the highest positive RIR (0.17 - 0.19) among the AVOCs, suggesting that the photolysis and
 280 oxidation of acetaldehyde was a limiting factor for O₃ formation. The important role of carbonyl
 281 compounds in atmospheric photochemistry has also been reported in previous studies, contributing
 282 up to 59.3% to the O₃ formation in ambient environments in China, the United States, and Brazil
 283 (Qin et al., 2021; Liu et al., 2022a; Edwards et al., 2014). Alkanes and alcohols exhibited lower RIR
 284 values (0.02 - 0.04), despite their high mass concentrations.



285

286 Figure 3. Modelled RIRs for (a) major O₃ precursors and (b) the AVOCs groups during
 287 photochemically active daytime (08:00-16:00) in the selected periods. (AVOCs: anthropogenic
 288 VOCs, all measured VOCs except for isoprene)

289

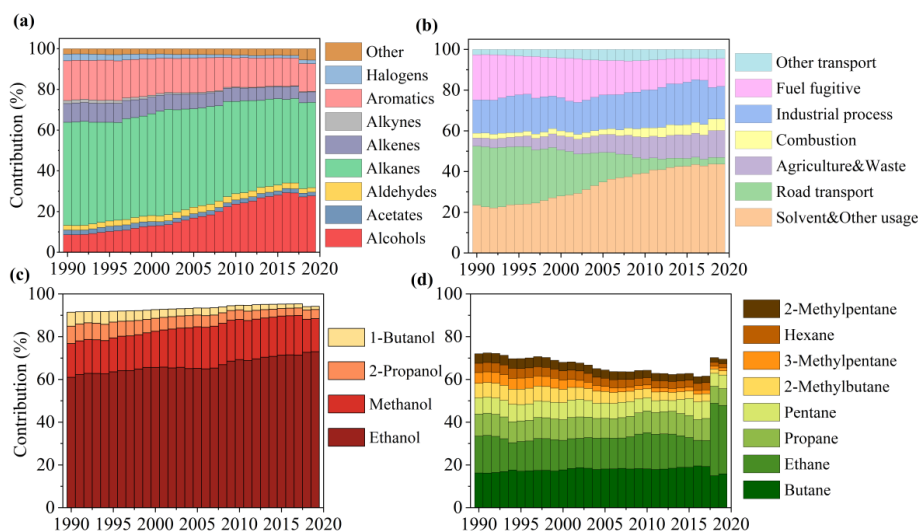
290 3.3 Emission inventory-informed O₃ production sensitivity tests

291 The trends in anthropogenic VOCs emissions from 1990 to 2019 estimated by the NAEI are
 292 shown in Figure S4. Over the period, the annual national emissions decreased by ~69.0% from 2,941
 293 kt in 1990 to 911kt in 2019. The reduction is partly attributed to more stringent controls for gasoline
 294 vehicle emissions, both tailpipe and evaporative/fugitive. In 2019, VOCs emissions from on-road
 295 transport and fuel fugitive losses accounted for only 3.3% and 13.7% of the total mass of VOCs
 296 emissions, compared to 29.1% and 26.9% in 1990. Efforts have also been directed towards



297 controlling industrial processes, commercial solvent usage, and combustion emissions, resulting in
298 reductions of 66.8%, 48.9%, and 20.7%, respectively over the period. However, contributions from
299 solvent usage to total VOCs emissions over 1990-2019 showed only modest reductions in the 1990s
300 and 2000s and indeed small increases in the most recent years (Figure 4(b)). This slight growth in
301 the solvent usage is due to increasing emissions from solvent use in consumer products such as
302 decorative products, aerosols, personal-care products, and detergents (NAEI, 2021). Solvent usage
303 had become the largest contributory sector (33.7%) to VOCs emissions by 2019, followed by
304 industrial processes (16.0%).

305 As shown in Figure 4(a), the VOC speciation over the 1990-2019 period was dominated in mass
306 terms by contributions from alkanes and alcohols, the former decreasing as gasoline sources
307 declined, the other increasing as non-industrial solvent and food and drink industry processes
308 emissions followed a different pattern. Alkane emissions fell from 46.6% to 30.6% over the period.
309 Further reductions in alkane emissions are expected due to the policies for phasing-out sales of new
310 internal combustion engine vehicles in the UK (and in many other places) by 2030 or 2035. Growth
311 in the relative contributions of alcohols was primarily driven by increases in emissions of methanol
312 and ethanol, and to a lesser extent in 1-butanol and 2-propanol (Figure 4(c)).



313
314 Figure 4. Contributions to annual national UK emissions of VOCs between 1990-2019 by: (a)
315 functional group; (b) by major emissions reporting sector; (c) for four individual alcohols in the
316 overall sub-class of alcohols; (d) for eight individual alkanes in the sub-class of all alkanes.



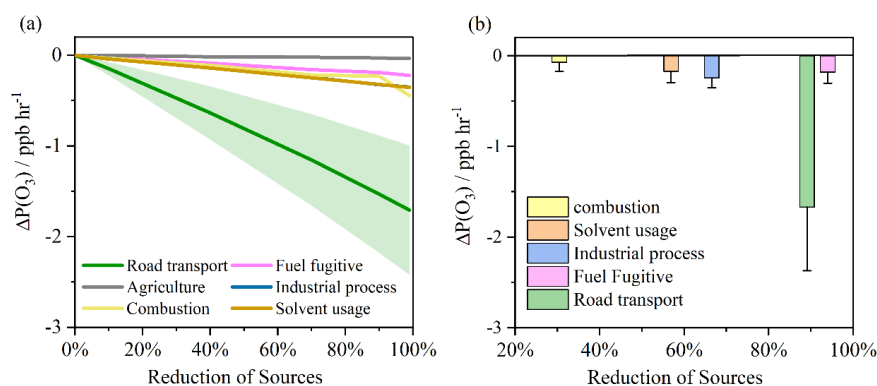
317 The NO_x, CO, and VOC speciation within the NAEI for each of the six major emission sectors
318 was used to assign proportional sectoral contributions to the VOCs observed in Birmingham, and
319 hence to ozone production in the case study. (Table S2). The six sectors are: road transport (both of
320 on-road exhaust emission and evaporative losses of fuel vapor), industrial processes, combustion,
321 solvent usage, fuel fugitive, and agriculture emissions). This makes a key assumption that the VOCs
322 at the observation site are affected directly in the same proportion that VOCs are reported in national
323 amounts in the NAEI. We make this assumption since it provides a reasonable starting point for
324 understanding how each VOC sector may influence O₃ production during a case study event,
325 however ozone formation might as well be sensitive to any differing regional distribution of
326 emission speciation.

327 Figure S5 shows the modelled RIRs for these sources in the initial, O₃, and clear-out periods.
328 All the sources generally showed higher RIR values in the O₃ period. Road transport exhibited the
329 highest positive RIR values in all periods (0.30 - 0.36), followed by industrial process (0.06 - 0.09)
330 and solvent usage (0.05 - 0.07). Despite being a relatively minor contributor to the mass of national
331 VOCs emissions (only 3.3% of the total in 2019), road transport VOCs still played the most
332 important role in local ozone photochemical chemistry, in this case study.

333 Figure 5a shows the changes in P(O₃) during the O₃ period from 08:00 to 16:00 which might
334 arise as a result of reductions in the individual sectors described above. This is a ‘thought experiment’
335 where under 2019 general observed atmospheric conditions (e.g., for NO_x, CO and so on), each of
336 the VOC source sectors is then further reduced in isolation (from 2019 levels) and the effects on
337 $\Delta P(O_3)$ were evaluated. Based on these scenarios, reducing emissions from the individual sectors
338 all resulted in decreased P(O₃), as would be anticipated. Reducing ozone precursors arising from
339 road transport would lead to a decreased P(O₃) of ~1.71 ppbv h⁻¹ if that sector could be 100% abated
340 in the case study. This is expected because road transport is a source of photochemically reactive
341 VOCs, species including aromatics, aldehyde, and short-chain alkanes/alkenes. Other sectors
342 showed more modest effects, with reductions in solvent-related VOCs the next most significant
343 lever to control ozone. Fully abating emissions of all industrial and solvent process emissions only
344 resulted in a decreased P(O₃) of ~0.35 ppbv h⁻¹, largely because they are dominated by ethanol and
345 methanol with relatively low RIR values. Considering the real-world changes in VOC emissions
346 over the period of 1990 to 2019, the very major reductions in road transport emissions have led to



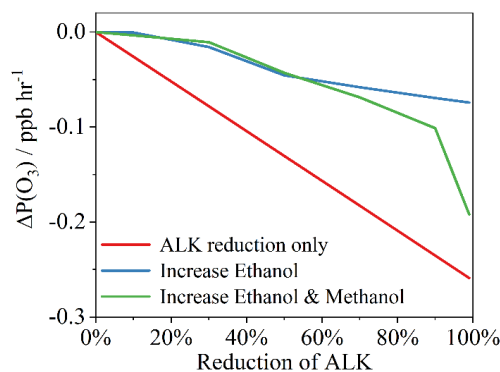
347 the largest effects in reducing $P(O_3)$ (Figure 5(b)). Whilst there have also been some very large
 348 reductions (94.6%) in fuel fugitive emissions, the impact on $P(O_3)$ reduction is modelled to have
 349 been relatively modest, being similar to industrial processes and solvent usage.



350

351 Figure 5. (a) Changes in $P(O_3)$ in response to different reductions in VOCs, NO_x , and CO from
 352 different sectors for the Birmingham-case study condition. (b) Changes in $P(O_3)$ based on the NAEI
 353 estimated reductions in VOCs from different sectors between 1990 and 2019. The standard
 354 deviations represent variability in $\Delta P(O_3)$ during 08:00-16:00 LST in the O_3 period.

355 Further model runs were performed to better understand the impacts of the shift between
 356 alkanes and alcohol species on $P(O_3)$, given trends showing decreasing alkanes emissions and
 357 increasing alcohol emissions between the 1990-2019 period (Figure 4). The modelled alkane
 358 concentrations in the case study were reduced by 10%, 30%, 50%, 70%, 90%, and 99%. This
 359 represents a downward trajectory in alkane emissions that would be anticipated as gasoline vehicles
 360 are slowly retired. Two further scenarios were then developed to sit alongside these reductions in
 361 alkanes. Firstly, the concentration of ethanol was increased to keep the overall total VOCs
 362 concentration in the model under case study conditions unchanged. Second, the concentration of
 363 both ethanol and methanol scaled upwards to keep total VOCs concentration unchanged. As shown
 364 in Figure 6, reductions in alkanes alone resulted in decreased $P(O_3)$ to a maximum of $\sim 0.26\ ppbv\ h^{-1}$
 365 if fully abated. If that alkane reduction was balanced with increased ethanol and methanol, then
 366 $P(O_3)$ is reduced by a maximum of $0.19\ ppbv\ h^{-1}$. If alkane reductions were balanced by increasing
 367 ethanol alone, then $P(O_3)$ still decreases, but only up to $0.07\ ppbv\ h^{-1}$.



368

369 Figure 6. Reductions in $\Delta P(O_3)$ based on reducing alkanes (ALK) in the model (under case study
370 conditions), reducing alkanes but balancing overall VOCs amount with increased ethanol (blue line)
371 and reducing alkanes but balancing overall VOCs amount with increased ethanol and methanol
372 (green line).

373

374 Conclusion

375 In this study, a typical high- O_3 event in Birmingham, United Kingdom during August 2022
376 was chosen as a case study to investigate the impacts of changes to VOCs emissions and speciation
377 on urban O_3 production. The *in-situ* O_3 formation sensitivity was split into three periods: initial,
378 high O_3 , and clear-out. Results from OH reactivity, O_3 budgets, and RIR index showed that O_3
379 formation in all three periods was impacted by both VOCs and NO_x , but was more sensitive to
380 anthropogenic VOCs. The oxidation of alcohols and photolysis of acetaldehyde substantially
381 contributed to *in-situ* O_3 formation, especially in the high O_3 period. The roles of anthropogenic
382 VOC sources in urban O_3 chemistry were examined by integrating the national atmospheric
383 emission inventory speciation over the period of 1990-2019 into photochemical box model
384 scenarios. Despite road transport only contributing 3.3% of national VOCs emissions in 2019, it still
385 played the most important VOC role in the case study ozone photochemistry, when inventory
386 contributions were mapped onto observed VOCs. Sequentially the observed VOCs were reduced by
387 the fractional contributions and speciation in the NAEI for six sectors to evaluate what impact
388 abating different VOCs-emitting sectors would have on $P(O_3)$. Abating road transport VOCs in
389 isolation would lead to a decreased $P(O_3)$ by up to 1.67 ppbv h^{-1} , but abating other sectors such as
390 solvent use and fugitive fuels had noticeably smaller effects. Despite emissions of VOCs from road



391 transport falling very dramatically between 1990 and 2019, it remains one of the most powerful
392 means to further reduce ozone in this typical UK case study. The wider shift in speciation reported
393 in the NAEI from alkane to alcohols was also examined using scenarios where emission reductions
394 for alkane, were counterbalanced with increases in alcohols, all simulated for the Birmingham
395 atmospheric case study conditions (e.g., for NO_x, CO and etc). Further reducing alkanes from
396 present day conditions to zero has a clear beneficial effect on reducing P(O₃) by up to ~0.26 ppb hr
397 ¹. However, this benefit could to a degree be offset should alcohol emissions (for example from non-
398 industrial solvent use) increase and counterbalance those alkane reductions. Whilst simple alcohols
399 are inherently less potent ozone-forming VOCs compared to the mixture of VOCs from road
400 transport, avoiding future growth in emissions remains important, since they weaken the long-term
401 benefits of road transport electrification and the phase out of internal combustion engine vehicles.

402

403 **Data Availability**

404 Observational data including meteorological parameters and air pollutants used in this study are
405 available at https://github.com/nervouslee/Birmingham_CS.git. UK national emission inventory is
406 available at <https://naei.beis.gov.uk/>.

407

408 **Author Contribution**

409 Jianghao Li prepared the manuscript with contributions from all authors. Alastair C. Lewis helped
410 with modelling scenarios and revised the manuscript. Jim R. Hopkins contributed to measurement
411 of chemical species. Stephen J. Andrews contributed to scientific discussion on findings of this work.
412 Tim Murrells, Neil Passant and Ben Richmond contributed to the data of national emission inventory
413 data and revision on NAEI methodology. Siqi Hou, Roy Harrison, and Zongbo Shi provided
414 measurements of atmospheric pollutants used in this study, along with critical discussion on revising
415 the manuscript.

416

417 **Competing interests**

418 The authors declare that they have no conflict of interest.

419



420 Acknowledgements

421 Establishment and operation of the Birmingham Air Quality Supersite operation (BAQS) is
422 supported by the NERC WM-Air project (NE/S003487/1) and UKRI Clean Air SPF project OSCA
423 (NE/T001976/1). This work forms part of the National Centre for Atmospheric Science National
424 Capability programme funded by NERC. Jianghao Li's study at University of York is financially
425 supported by the China Scholarship Council.

426

427 References

428

- 429 Abernethy, S., O'Connor, F., Jones, C., and Jackson, R.: Methane removal and the proportional reductions
430 in surface temperature and ozone, *Philosophical Transactions of the Royal Society A*, 379,
431 20210104, 10.1098/rsta.2021.0104, 2021.
- 432 Air Quality Expert Group, Non-methane Volatile Organic Compounds in the UK: [https://uk-
433 air.defra.gov.uk/library/reports.php?report_id=10032020](https://uk-air.defra.gov.uk/library/reports.php?report_id=10032020), last access: 07 September 2023.
- 434 Calvert, J. G., Orlando, J. J., Stockwell, W. R., and Wallington, T. J.: The mechanisms of reactions
435 influencing atmospheric ozone, Oxford University Press, USA, 2015.
- 436 Chen, T., Xue, L., Zheng, P., Zhang, Y., Liu, Y., Sun, J., Han, G., Li, H., Zhang, X., and Li, Y.: Volatile
437 organic compounds and ozone air pollution in an oil production region in northern China,
438 *Atmospheric Chemistry and Physics*, 20, 7069-7086, 10.5194/acp-20-7069-2020, 2020.
- 439 Cliff, S. J., Lewis, A. C., Shaw, M. D., Lee, J. D., Flynn, M., Andrews, S. J., Hopkins, J. R., Purvis, R.
440 M., and Yeoman, A. M.: Unreported VOC emissions from road transport including from electric
441 vehicles, *Environmental science & technology*, 10.1021/acs.est.3c00845, 2023.
- 442 Coggon, M. M., Gkatzelis, G. I., McDonald, B. C., Gilman, J. B., Schwantes, R. H., Abuhassan, N.,
443 Aikin, K. C., Arend, M. F., Berkoff, T. A., Brown, S. S., Campos, T. L., Dickerson, R. R., Gronoff,
444 G., Hurley, J. F., Isaacman-VanWertz, G., Koss, A. R., Li, M., McKeen, S. A., Moshary, F., Peischl,
445 J., Pospisilova, V., Ren, X., Wilson, A., Wu, Y., Trainer, M., and Warneke, C.: Volatile chemical
446 product emissions enhance ozone and modulate urban chemistry, *Proc Natl Acad Sci U S A*, 118,
447 10.1073/pnas.2026653118, 2021.
- 448 de Foy, B., Brune, W. H., and Schauer, J. J.: Changes in ozone photochemical regime in Fresno,
449 California from 1994 to 2018 deduced from changes in the weekend effect, *Environmental Pollution*,
450 263, 114380, 10.1016/j.envpol.2020.114380, 2020.
- 451 Department for Environment, Food & Rural Affairs. An annual update of data on concentrations of major
452 air pollutants in the UK: [https://www.gov.uk/government/statistical-data-sets/env02-air-quality-
453 statistics](https://www.gov.uk/government/statistical-data-sets/env02-air-quality-statistics), last access: 07 September 2023.
- 454 Diaz, F. M., Khan, M. A. H., Shallcross, B. M., Shallcross, E. D., Vogt, U., and Shallcross, D. E.: Ozone
455 trends in the United Kingdom over the last 30 years, *Atmosphere*, 11, 534, 10.3390/atmos11050534,
456 2020.
- 457 Edwards, P. M., Brown, S. S., Roberts, J. M., Ahmadov, R., Banta, R. M., deGouw, J. A., Dube, W. P.,
458 Field, R. A., Flynn, J. H., Gilman, J. B., Graus, M., Helmig, D., Koss, A., Langford, A. O., Lefter, B.



- 459 L., Lerner, B. M., Li, R., Li, S. M., McKeen, S. A., Murphy, S. M., Parrish, D. D., Senff, C. J., Soltis,
460 J., Stutz, J., Sweeney, C., Thompson, C. R., Trainer, M. K., Tsai, C., Veres, P. R., Washenfelder, R.
461 A., Warneke, C., Wild, R. J., Young, C. J., Yuan, B., and Zamora, R.: High winter ozone pollution
462 from carbonyl photolysis in an oil and gas basin, *Nature*, 514, 351-354, 10.1038/nature13767, 2014.
463 European Environment Agency.: EMEP/EEA air pollutant emission inventory guidebook 2016, 2016.
464 <https://www.eea.europa.eu/publications/emep-eea-guidebook-2016>, last access 07 September 2023.
465 Gaudel, A., Cooper, O. R., Chang, K.-L., Bourgeois, I., Ziemke, J. R., Strode, S. A., Oman, L. D., Sellitto,
466 P., Nédélec, P., Blot, R., Thouret, V., and Granier, C.: Aircraft observations since the 1990s reveal
467 increases of tropospheric ozone at multiple locations across the Northern Hemisphere, *Science*
468 *Advances*, 6, eaba8272, doi:10.1126/sciadv.aba8272, 2020.
469 Gkatzelis, G. I., Coggon, M. M., McDonald, B. C., Peischl, J., Aikin, K. C., Gilman, J. B., Trainer, M.,
470 and Warneke, C.: Identifying volatile chemical product tracer compounds in US cities,
471 *Environmental Science & Technology*, 55, 188-199, 10.1021/acs.est.0c05467, 2020.
472 He, Z., Wang, X., Ling, Z., Zhao, J., Guo, H., Shao, M., and Wang, Z.: Contributions of different
473 anthropogenic volatile organic compound sources to ozone formation at a receptor site in the Pearl
474 River Delta region and its policy implications, *Atmospheric Chemistry and Physics*, 19, 8801-8816,
475 10.5194/acp-19-8801-2019, 2019.
476 Ivatt, P. D., Evans, M. J., and Lewis, A. C.: Suppression of surface ozone by an aerosol-inhibited
477 photochemical ozone regime, *Nature Geoscience*, 15, 536-540, 2022.
478 Jenkin, M., Saunders, S., Wagner, V., and Pilling, M.: Protocol for the development of the Master
479 Chemical Mechanism, MCM v3 (Part B): tropospheric degradation of aromatic volatile organic
480 compounds, *Atmospheric Chemistry and Physics*, 3, 181-193, 10.5194/acp-3-181-2003, 2003.
481 Kumar, P., Kuttippurath, J., von der Gathen, P., Petropavlovskikh, I., Johnson, B., McClure-Begley, A.,
482 Cristofanelli, P., Bonasoni, P., Barlasina, M. E., and Sanchez, R.: The Increasing Surface Ozone and
483 Tropospheric Ozone in Antarctica and Their Possible Drivers, *Environ Sci Technol*, 55, 8542-8553,
484 10.1021/acs.est.0c08491, 2021.
485 Lee, J. D., Drysdale, W. S., Finch, D. P., Wilde, S. E., and Palmer, P. I.: UK surface NO₂ levels dropped
486 by 42% during the COVID-19 lockdown: impact on surface O₃, *Atmospheric Chemistry and Physics*,
487 20, 15743-15759, 10.5194/acp-20-15743-2020, 2020.
488 Lefohn, A. S., Malley, C. S., Smith, L., Wells, B., Hazucha, M., Simon, H., Naik, V., Mills, G., Schultz,
489 M. G., Paoletti, E., De Marco, A., Xu, X., Zhang, L., Wang, T., Neufeld, H. S., Musselman, R. C.,
490 Tarasick, D., Brauer, M., Feng, Z., Tang, H., Kobayashi, K., Sicard, P., Solberg, S., and Gerosa, G.:
491 Tropospheric ozone assessment report: Global ozone metrics for climate change, human health, and
492 crop/ecosystem research, *Elementa: Science of the Anthropocene*, 6, 10.1525/elementa.279, 2018.
493 Lewis, A. C., Hopkins, J. R., Carslaw, D. C., Hamilton, J. F., Nelson, B. S., Stewart, G., Dorn, J.,
494 Passant, N., and Murrells, T.: An increasing role for solvent emissions and implications for future
495 measurements of volatile organic compounds, *Philosophical Transactions of the Royal Society A*,
496 378, 20190328, 10.1098/rsta.2019.0328, 2020.
497 Li, J., Yu, Z., Du, Z., Ji, Y., and Liu, C.: Standoff chemical detection using laser absorption spectroscopy:
498 a review, *Remote Sensing*, 12, 2771, 10.3390/rs12172771, 2020.
499 Liu, Q., Gao, Y., Huang, W., Ling, Z., Wang, Z., and Wang, X.: Carbonyl compounds in the atmosphere:
500 A review of abundance, source and their contributions to O₃ and SOA formation, *Atmospheric*
501 *Research*, 106184, 10.1016/j.atmosres.2022.106184, 2022a.
502 Liu, T., Hong, Y., Li, M., Xu, L., Chen, J., Bian, Y., Yang, C., Dan, Y., Zhang, Y., and Xue, L.:



- 503 Atmospheric oxidation capacity and ozone pollution mechanism in a coastal city of southeastern
504 China: analysis of a typical photochemical episode by an observation-based model, *Atmospheric*
505 *Chemistry and Physics*, 22, 2173-2190, 10.5194/acp-22-2173-2022, 2022b.
- 506 McDonald, B. C., De Gouw, J. A., Gilman, J. B., Jathar, S. H., Akherati, A., Cappa, C. D., Jimenez, J. L.,
507 Lee-Taylor, J., Hayes, P. L., and McKeen, S. A.: Volatile chemical products emerging as largest
508 petrochemical source of urban organic emissions, *Science*, 359, 760-764, 10.1126/science.aaq0524,
509 2018.
- 510 National Atmospheric Emissions Inventory.: UK Informative Inventory Report (1990 to 2019), 2021.
511 https://naei.beis.gov.uk/reports/reports?report_id=1016, last access 07 September 2023.
- 512 Nelson, B. S., Stewart, G. J., Drysdale, W. S., Newland, M. J., Vaughan, A. R., Dunmore, R. E., Edwards,
513 P. M., Lewis, A. C., Hamilton, J. F., and Acton, W. J.: In situ ozone production is highly sensitive to
514 volatile organic compounds in Delhi, India, *Atmospheric Chemistry and Physics*, 21, 13609-13630,
515 10.5194/acp-21-13609-2021, 2021.
- 516 Qin, M., Murphy, B. N., Isaacs, K. K., McDonald, B. C., Lu, Q., McKeen, S. A., Koval, L., Robinson,
517 A. L., Efstathiou, C., and Allen, C.: Criteria pollutant impacts of volatile chemical products
518 informed by near-field modelling, *Nature sustainability*, 4, 129-137, 10.1038/s41893-020-00614-1,
519 2021.
- 520 Saunders, S. M., Jenkin, M. E., Derwent, R., and Pilling, M.: Protocol for the development of the Master
521 Chemical Mechanism, MCM v3 (Part A): tropospheric degradation of non-aromatic volatile organic
522 compounds, *Atmospheric Chemistry and Physics*, 3, 161-180, 10.5194/acp-3-161-2003, 2003.
- 523 Seinfeld, J. H. and Pandis, S. N.: *Atmospheric chemistry and physics: from air pollution to climate*
524 *change*, John Wiley & Sons, 2016.
- 525 Sicard, P.: Ground-level ozone over time: an observation-based global overview, *Current Opinion in*
526 *Environmental Science & Health*, 19, 100226, 10.1016/j.eti.2022.102809, 2021.
- 527 Tarasick, D., Galbally, I. E., Cooper, O. R., Schultz, M. G., Ancellet, G., Leblanc, T., Wallington, T. J.,
528 Ziemke, J., Liu, X., and Steinbacher, M.: Tropospheric Ozone Assessment Report: Tropospheric
529 ozone from 1877 to 2016, observed levels, trends and uncertainties, *Elem Sci Anth*, 7, 39,
530 10.1525/elementa.376, 2019.
- 531 Wang, Y., Guo, H., Zou, S., Lyu, X., Ling, Z., Cheng, H., and Zeren, Y.: Surface O₃ photochemistry over
532 the South China Sea: Application of a near-explicit chemical mechanism box model, *Environmental*
533 *Pollution*, 234, 155-166, 10.1016/j.envpol.2017.11.001, 2018.
- 534 Warburton, T., Grange, S. K., Hopkins, J. R., Andrews, S. J., Lewis, A. C., Owen, N., Jordan, C.,
535 Adamson, G., and Xia, B.: The impact of plug-in fragrance diffusers on residential indoor VOC
536 concentrations, *Environmental Science: Processes & Impacts*, 25, 805-817, 10.1039/D2EM00444E,
537 2023.
- 538 Winkler, S., Anderson, J., Garza, L., Ruona, W., Vogt, R., and Wallington, T.: Vehicle criteria pollutant
539 (PM, NO_x, CO, HCs) emissions: how low should we go?, *Npj Climate and atmospheric science*, 1,
540 26, 10.1038/s41612-018-0037-5, 2018.
- 541 Wolfe, G. M., Marvin, M. R., Roberts, S. J., Travis, K. R., and Liao, J.: The framework for 0-D
542 atmospheric modeling (F0AM) v3. 1, *Geoscientific Model Development*, 9, 3309-3319,
543 10.5194/gmd-9-3309-2016, 2016.
- 544 Wu, R. and Xie, S.: Spatial Distribution of Ozone Formation in China Derived from Emissions of
545 Speciated Volatile Organic Compounds, *Environ Sci Technol*, 51, 2574-2583,
546 10.1021/acs.est.6b03634, 2017.



547 Yeoman, A. M. and Lewis, A. C.: Global emissions of VOCs from compressed aerosol products, Elem
548 Sci Anth, 9, 00177, 10.1525/elementa.2020.20.00177, 2021.
549 Zulkifli, M. F. H., Hawari, N. S. S. L., Latif, M. T., Abd Hamid, H. H., Mohtar, A. A. A., Idris, W. M. R.
550 W., Mustafa, N. I. H., and Juneng, L.: Volatile organic compounds and their contribution to ground-
551 level ozone formation in a tropical urban environment, Chemosphere, 302, 134852,
552 10.1016/j.chemosphere.2022.134852, 2022.
553